

# Privacy-Preserving Performance Profiling of In-The-Wild GPUs

Ian McDougall<sup>1</sup>, Michael Davies<sup>2</sup>, Rahul Chatterjee<sup>1</sup>, Somesh Jha<sup>1</sup>, and Karthikeyan Sankaralingam<sup>1</sup>

<sup>1</sup>University of Wisconsin-Madison

<sup>2</sup>NVIDIA Research

September 29, 2025

## Abstract

GPUs are the dominant platform for many important applications today including deep learning, accelerated computing, and scientific simulation. However, as the complexity of both applications and hardware increases, GPU chip manufacturers face a significant challenge: how to gather comprehensive performance characteristics and value profiles from GPUs deployed in real-world scenarios. Such data, encompassing the types of kernels executed and the time spent in each, is crucial for optimizing chip design and enhancing application performance. Unfortunately, despite the availability of low-level tools like NSYS and NCU, current methodologies fall short, offering data collection capabilities only on an individual user basis rather than a broader, more informative fleet-wide scale. This paper takes on the problem of realizing a system that allows planet-scale real-time GPU performance profiling of low-level hardware characteristics. The three fundamental problems we solve are: i) user experience of achieving this with no slowdown; ii) preserving user privacy, so that no 3rd party is aware of what applications any user runs; iii) efficacy in showing we are able to collect data and assign it applications even when run on 1000s of GPUs. Our results simulate a 100,000 size GPU deployment, running applications from the Torchbench suite, showing our system addresses all 3 problems.

## 1 Introduction

GPUs are the dominant platform for many important applications today including deep learning [51], accelerated computing, and scientific simulation [21]. However, as the complexity of both applications and hardware increases (the recent Hopper GPU includes sophisticated components like a tensor memory accelerator, support for atomics, and the latest generation TensorCore [15, 58]), GPU chip manufacturers face a significant challenge: *how to gather comprehensive performance characteristics from GPUs deployed in real-world scenarios*. Despite the availability of low-level tools like NSYS and NCU [57], current methodologies fall short, offering data collection capabilities only on an individual user basis rather than a broader, more informative planet-wide scale.

This paper argues for the necessity of a new paradigm in GPU performance data collection, envisioning a form of statistical debugging or continuous planet-wide profiling. Our primary inspiration is Google-Wide Profiling [40] which unearthed a wealth of data that drove data-center design. The authors in their recent retrospective emphasize that: “Finally, fleetwide profiling is considered standard in hyperscalars today — there is little doubt about the benefits of finding optimization opportunities with live traffic.” A subtle but important difference is that our goal is to make this data available to chip developers as opposed to a hyperscalar’s “in-



Figure 1: Penrose Components

### ternal” use and characterization.

*This paper envisions to collect low-level performance counter data from deployed GPUs across a large number of users while causing negligible interference to or detraction of the user experience. The recipients of this profiling data are **chip designers** to improve the performance of GPUs.*

Achieving this vision involves several key challenges, particularly in the areas of observability, privacy, and efficient data management. In this context, observability refers to which performance counters can be monitored and how accurately they reveal the running application. The data then should be collected by the chip designers for further analysis. This data collection and aggregation must be done in a way that preserve the privacy of the user applications. Existing solutions [30, 20, 3, 50, 23, 31, 73, 17, 74] fall short in two major ways: they lack privacy-preserving methods for users to share performance data with **chip manufacturers**, and they do not enable manufacturers to effectively analyze data from diverse sources without compromising user privacy (more in § 3.4).

Addressing these aforementioned three challenges, this paper introduces a three-pronged solution designed to work seamlessly with state-of-the-art unmodified GPU hardware deployments and off-the-shelf software. Our overall system, called Penrose, is outlined in Figure 1. Penrose introduces an untrusted (honest-but-curious) aggregation server (AS) which receives encrypted data directly from GPUs, aggregates them, and only shares the encrypted aggregated data with the chip designers (designer servers or DS). The AS can be hosted on public cloud services such as Azure, GCP, AWS, or Equinix and run by an organization separate from DS. Second, our solution incorporates Additive Homomorphic Encryption (AHE)<sup>1</sup> — through careful system design, only

additions on encrypted data are needed to process data on untrusted third-party servers, ensuring that DS can gain insights without ever accessing raw user data directly, while preventing the AS from learning anything about the hardware performance counter data or individual users who are participating in Penrose. We develop an automatic application identification and classification approach. Penrose uses extremely low sampling rates combined with wide-scale execution to achieve speed and coverage across applications. To concretize the solution, we focus on workstation/data-center class GPUs, although the principles translate to other accelerators (e.g. accelerators on mobile devices’ or autonomous vehicles’ SoCs), FPGAs, and CPUs. In practice, we show that a single aggregation server on a m3.small.x86 Equinix instance with a 25 Gbps network link can easily service 100,000 GPUs — the cost of such a deployment is approximately \$6000 per year [26]. Penrose’s aggregated per-performance counter histograms are extremely useful to chip designers, they can examine how intensely different hardware units (e.g., tensor cores, caches, memory bandwidth) are exercised under the applications run in-the-wild as opposed to benchmarks, or limited in-house characterization and study of some workloads.

To evaluate Penrose, we used a hybrid approach that includes measurements on real hardware considering the entire Torchbench suite (150+ applications), an implementation of AHE aggregation using the Paillier library [38], and network traffic measurements. We built a Penrose planet-scale simulator that simulates GPU deployment at scale to study coverage, time to collect data, network effects, and cost effectiveness. This paper’s contributions are:

- Design of the Penrose system that allows at-speed planet-wide GPU performance profiling without any hardware modifications.
- A novel histogram aggregation algorithm using partial homomorphic accumulation on encrypted data to provide user privacy and allowing only chip designers to access performance data.
- A formalization of Penrose’s privacy guarantees

<sup>1</sup>Although fully homomorphic encryption allows performing any operation over encrypted data, it is computationally very

expensive, while a restriction to addition provides a variety of other simpler and faster solutions [2].

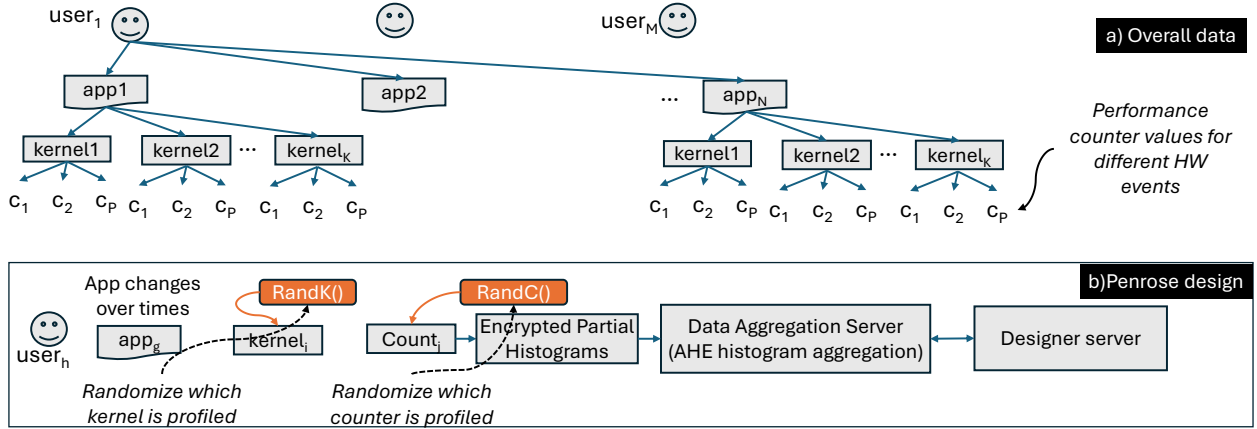


Figure 2: Penrose conceptual overview

under a practical threat model we describe.

- Simulation-based results that show Penrose is effective; it obtains over 99% application coverage within 8 hours, when running across 100,000 GPUs, needing a single aggregation server, and has an average slowdowns of 0.045%. Penrose’s design can be scaled-out to support millions of GPUs by adding more aggregation servers.

Paper organization: §2 provides an overview of Penrose, §3 provides its detailed design, §4 discusses evaluation methodology, §5 presents our results, §6 discusses related work, and §7 concludes.

## 2 Penrose Overview

We aim to design a profiling system for GPUs. In the context of GPUs, an “ideal system” would enable global capturing of all performance counters for every application and GPU-kernel running on real end-user systems with no perceivable user slowdown and no breach of user privacy. Given  $P$  performance counters, we want a distribution (or min, max, average) for every value aggregated across all instances of an application and for every GPU kernel (across all users). Given  $N$  total applications, this amounts to  $N \times P$  application histograms. We envision that these histograms would be analyzed by chip designers, and the server they run is called the designer server (DS). Figure 2(a) shows an abstract view of data generated

which is comprised of many users, and  $N$  applications, with each application essentially comprising of a set of GPU kernels, and for each kernel we want to capture  $P$  performance counters.

Penrose has three types of entities: (i) A set of *GPU users* who consented to participate in Penrose program, (ii) An *aggregation server* (AS) which will help aggregate information from GPU users before sharing them with the chip designer, and (iii) *chip designer* (DS), who receive the aggregated GPU telemetry data periodically from the AS. If we consider organizations like OpenAI running a software service on GPU that is then provided to customers, in our definition the user is OpenAI running GPU code in a cloud.

### 2.1 Strawman Solution and Challenges

A naive design to capture this data and create a profiling system can be designed using existing NVIDIA profiling tools, Nsight Systems (NSYS) and Nsight Compute (NCU) which interface with the CUDA profiling tools interface (CUPTI) to monitor GPU activity on all end-user GPUs (similar tools for AMD chips also exist, as do data-center variants like DCGM). A separate monitor process connects with these tools to collect performance counter data and transmits it to a database for collection and storage.

This strawman approach presents four (perhaps

obvious) challenges: **User Slowdown**: Sampling all kernels of an application would incur enormous slowdowns for users which would disrupt application runtime. Overall these range from  $2\times$  to  $10\times$  [57]. Collecting more than one performance counter (requiring kernel replay) introduces further slowdowns. **Data Overload**: Naively capturing data from all users all the time would vastly increase the storage and network requirements at the AS and for users. **Privacy Infringement**: Transmitting plaintext data to designers would violate user privacy, by revealing data such as what kernel or applications an individual user is running. Specifically our privacy goals are: keep what application an user runs private and keep kernel names a user runs private. The only information the designers get to see are *histograms* of performance counters for different applications (without knowing which application it is) across users. **Application Identification**: Given the GPU driver and hardware only sees a stream of kernels (i.e. application binary or Deep-learning model names are inaccessible), we need a way to identify different applications from kernel streams to enable application-level matching across users.

## 2.2 GPU application Identification

One of the key challenges in collecting GPU telemetry is the lack of a reliable application identifier. In the context of GPU computations, traditional identifiers, such as application names or binary names, are often not visible or accessible. Therefore, we need an alternative method to define and distinguish applications.

**Snippets.** To address this, we introduce the concept of a “snippet” as a way to identify and label applications. A *snippet* is a sequence of dynamic kernel invocations with a fixed maximum length (i.e. **snippet length**). Snippets are used to identify applications in the Penrose system in a manner that is oblivious to the original application name or software. A **Snippet Sequence** refers specifically to the full list of kernel names that make up the snippet. The snippet sequence is used to compare two snippets to determine whether they represent the same applica-

tion. In practice, as we show later for application anonymity, the snippet sequence is never transmitted in clear text to the AS or DS. Instead a min-hash (with 8-gram overlapping kernels and 100 hash functions) is sent to the AS. We call this a **Snippet Sequence Min-Hash**. A **Canonical Sequence Min-Hash Snippet** or simply Canonical Snippet is a representative snippet that is used to identify one application. Min-hash belongs in the family of locality sensitive hashing allowing similar hashes to be compared to determine if their unhashed contents was originally similar. A **Snippet Hash** is a hash of the snippet sequence min-hash that is used for lookup to determine exact matches to avoid more costly sequence comparisons. The DS only receives Snippet Hashes. Consider a sequence of kernels of length 10 — AAABCCDDDE, where letters denote kernel names. Applying overlapping 8-grams on this with 100 hash functions produces a 100 64-bit values which would be the Snippet Sequence Min-Hash. A 256-bit SHA2 hash of these 100 values is the Snippet Hash. A *public application* is one which the AS or DS has access to in binary form. For these, the AS can learn the snippet sequence from the code or application binaries trivially - the AS can use tools like `nsys` and other NSIGHT tools [19] to obtain a trace of kernels. *Private applications* are one’s whose binary or source-code is not available to the AS or DS.

## 2.3 Privacy requirements and design

In § 3.3, we will detail how our design of Penrose ensures the security and privacy properties we outline below.

**Threat model.** In our threat model, we assume all participating parties are honest-but-curious (also sometimes known as the semi-honest model), thus they will follow the protocol specified in Penrose, but might try to glean information from the data they receive. Specifically, we assume AS and DS do not collude or share information that is not specified in the protocol. This is a widely used model for creating practical and deployable secure systems [60, 7], in particular Apple’s deployed protocol for private set intersection (PSI) uses this threat model.

*Security goals.* Informally, we want to ensure

that *only* the DS learns the aggregate snippet histograms of different applications run by Penrose participants and no one learns which applications a participating user is running. We formalize this into three classes of security and privacy guarantees: (1) **User anonymity:** Given a set of encrypted partial histogram update messages and a user identity, say an IP address, AS should not be able to identify if any of the messages originated from the user identity. This means that AS or DS should not be able to tell whether or not a particular user (identified their IP address) contributed any histogram in a round of data aggregation. (2) **Application confidentiality:** AS or DS must not be able to learn the sequence of kernels involved in a *private application* run by a user who has opted into Penrose. (3) **Histogram confidentiality:** AS cannot learn anything about the partial histograms of the performance counters and DS only learns the aggregate histograms, aggregated over a specified time period.

*Acceptable information leakage.* AS and DS are allowed to learn how often an application (identified simply by its snippet-hash, and not binary name etc.) is executed among the users who opted into Penrose. As users opt into Penrose, we do not consider whether a user opts into Penrose or not as a secret information. Although the AS and DS do not learn any user identity, other entities could try to infer whether a user participates in Penrose by, say, monitoring their network activity. Finally, Penrose does not attempt to protect the sequence of kernels present in a public GPU application.

## 2.4 Penrose Solution

The Penrose system solves all four problems described in § 2.1 by implementing a scalable and privacy-preserving framework that is able to profile kernels and entire applications as shown in Figure 2(b). To mitigate user-slowdown, Penrose applies sampling at the individual chip level to capture only a subset of kernels and performance counter data, relying on a large number of users running popular applications many times with randomized sampling to build a complete picture of each application and its kernels. To reduce and handle the massive amount of data produced by capturing a range of

performance counters for all applications and kernels, Penrose aggregates multiple samples across users for the application into per-counter histograms, dramatically reducing the per-chip storage requirements. To preserve user privacy, Penrose hashes kernel names for anonymity before transmitting data to the Aggregating Server (AS). It also employs additive homomorphic encryption (AHE) to securely perform histogram aggregation. Additionally, all communication between users and the AS is routed through an anonymity network such as Tor (see § 3.3 for more details). This ensures that each user’s contribution to the aggregated histograms remains private and cannot be individually recovered.

To provide meaningful mapping between profiling data and anonymized applications, Penrose divides applications into snippets — sequences of dynamic kernel streams that identify each application. This allows the Penrose monitor to remain unaware of the high-level software driving execution while still associating kernel streams with specific applications in a privacy-preserving way. The DS receives encrypted aggregate histograms from the AS at regular intervals (or via queries) and decrypts them using its secret key. For this overview, assume we have a snippet table that groups similar snippets, deferring details of its construction (§ 3.1).

**Assumptions.** Penrose’s efficacy and cost effectiveness relies on two underlying assumptions, while we make a third assumption specific to our prototype. **(1) Number of Users:** A large number of users opting in to collect performance data is necessary for quick kernel and application coverage at low sampling rates. **(2) Hot applications:** In order to sample applications at a low rate and achieve good coverage in a reasonable amount of time, we assume that GPU applications consist of a number of frequently used apps. This assumption is also critical for accurate application identification. At the extreme, if every user runs a unique set of applications, the statistical nature of obtaining application coverage will break down. However, we show that our design can scale-out; to support more applications, more GPUs would need to opt-in to achieve convergence in the same amount of time (details are provided in § 5.7 including a uniform and normal distribution of application

usage). **(3) Platform-specificity:** The prototype of Penrose we built is for NVIDIA hardware using its profiling tools. However, the core ideas and the implementation can be easily adopted for other chip designers, such as AMD or Intel.

## 2.5 Why Planet-Scale Profiling?

We first articulate why a privacy-preserving, opt-in, global-scale GPU telemetry system is not just valuable—but necessary—for the future of chip design, around some core concerns.

**Open-Source AI is Not Enough.** While open-source AI models (e.g., LLaMA) are valuable, the most widely deployed and influential systems—including OpenAI’s GPT, Google’s Gemini, and Anthropic’s Claude—are closed-source. Their runtime behavior is opaque: critical architectural stressors like TensorCore saturation, memory bandwidth usage, and context-specific cache pressure cannot be inferred from APIs or academic benchmarks. Even when open-source models are used, deployment characteristics (e.g., batch sizes, prompt chaining, runtime quantization) vary widely across users. Penrose captures actual runtime behavior across this real-world heterogeneity—something no benchmark or public model trace can offer.

**Hyperscaler Profiling is Not Generalizable.** Hyperscaler profiling infrastructure (e.g., DCGM) serves internal optimization needs but is inaccessible, unshareable, and narrowly scoped: i) DCGM cannot aggregate workload behavior across organizations. ii) It lacks any privacy guarantees, making external adoption infeasible. iii) It assumes full visibility and control—conditions not available in public deployments. Penrose breaks this silo. It enables performance telemetry that is: i) Cross-organizational and planet-scale, ii) Privacy-preserving by design (via AHE + anonymity networks), iii) Opt-in, low-overhead, and iv) Decoupled from hyperscaler infrastructure. This creates the first viable path for participatory, user-respecting telemetry that chip designers can actually access.

**Workload Diversity is Real and Measurable, insights can guide hardware.** Figures 4 and 7 show that workloads exhibit significant heterogeneity.

Using traces from numerous applications, we observe that performance counters—including TensorCore usage and DRAM bandwidth—vary widely across users and time. The histogram data, reveals previously unknown insights. For instance, the prevalence of resource underutilization (e.g., TensorCores active while DRAM is idle): these results suggest optimization opportunities in overlapping execution phases.

**User Opt-In and Chipmaker Contract.** The assumption that users would consent to privacy-preserving telemetry is well grounded in modern computing practice. Operating systems like Windows, macOS, Android, and iOS routinely collect performance metrics, crash diagnostics, and usage analytics through opt-in telemetry. Tesla vehicles continuously transmit driving and sensor data to improve hardware and software reliability. Even in the hardware space, Intel’s Platform Monitoring Technology (PMT) and Telemetry Interface Specification (TIS) allow firmware-level performance data to be collected by OEMs or system administrators for system health and debugging purposes. What these systems lack—unlike Penrose—is a commitment to transparency, open aggregation, and cryptographic privacy protection. Penrose is designed to be explicitly opt-in, uses additive homomorphic encryption to ensure differential privacy at scale, and provides verifiable guarantees that user-level data is never exposed. Importantly, the benefit to users is tangible: for consumers, better performance, stability, and efficiency in future hardware tuned to real workloads; for enterprises, the ability to benchmark software in production-like conditions and influence vendor decisions on future architecture trade-offs. Penrose reimagines telemetry as a collaborative bridge between users and chipmakers in a rapidly evolving compute landscape.

## 2.6 Definition of Terms

We now discuss important terms used by the Penrose system. Table 1 (in page 14) describes all the parameters used by Penrose.

**Sampling and Aggregation.** Penrose will sample kernels periodically to reduce the overhead on

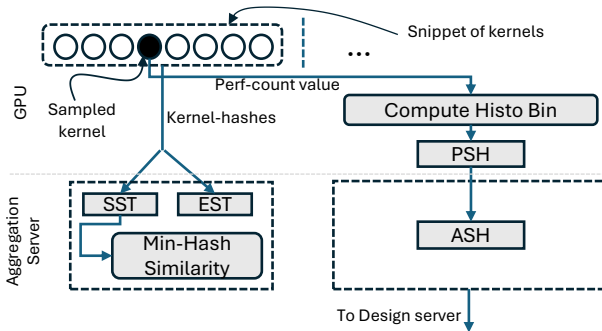


Figure 3: Dataflow from users to aggregation server.

the GPU performance. However, a uniform period of sampling could lead to bias in sampling, and only sample a small subset of all kernels executed on the GPU. Therefore, we will define two parameters to sample every  $S^{th}$  kernel, which is known as the **sampling interval**. A new sampling interval is selected every ( $O$ ) seconds known as **sampling reset interval**.

During profiling, the **aggregation threshold** ( $A$ ) determines the number of samples after which an application-level partial histograms are transmitted to the AS. The histograms generated by a user are referred to as **partial histograms**. The partial histograms are encrypted using an additively homomorphic encryption (AHE) scheme prior to transmitting over an anonymity network such as Tor (See § 3.3 for more details). AS aggregate the encrypted histograms by adding the encrypted histogram values and report to the DS every  $\delta$  minutes known as **server report interval**. The **aggregated snippet histogram (ASH)** refers to an aggregation of encrypted partial histograms maintained by the AS for a performance counter for a particular snippet across all users. Note by design of Penrose, AS cannot learn the plaintext histograms.

### 3 Penrose System Architecture

The Penrose system's operation is split between two logical phases: a snippet classification phase (§3.1) and a data collection phase (§3.2). We discuss how Penrose ensures user privacy in § 3.3. Figure 3 shows

information flow between the components of Penrose.

#### 3.1 Snippet classification

**Data Collection and Structure.** The client-side is responsible for generating a sequence of kernel names, – this information is directly available in the GPU driver. Once a sequence reaches the predetermined length  $L$ , or the application ends, it constitutes a complete snippet. The snippet is then transmitted to the AS. Note that clients only send Snippet Sequence Min-Hash and not the kernel names themselves to the AS (to preserve application anonymity). It also sends a SHA-256 hash of this min-hash. The AS maintains two key data structures: the snippet sequence table (SST), which stores each canonical snippet's snippet hash and snippet sequence min-hash, and the equivalent snippet table (EST), a hash table that maps every snippet hash to its canonical snippet hash, facilitating efficient management and retrieval. A snippet,  $\mathbf{K} = (k_1, k_2, \dots, k_n)$ , where each  $k_j$  is a kernel name.

**Client Role.** During program execution, clients assemble and send the snippet sequence min-hash of a snippet to the AS and it's a 256-bit hash. Upon receipt of a snippet sequence min-hash, the AS determines the corresponding canonical snippet. To compute a MinHash signature for a kernel sequence  $K$ , multiple hash functions are applied on overlapping 8-grams of  $K$ . Let the set of 8-grams of  $K$  be  $G(K)$ ; we then compute the MinHash for  $K$  as:

$$\text{MinHash}(K) = (\min\{h_j(g) \mid g \in G(K)\} \mid j = 1, 2, \dots, H)$$

where  $H = 100$  is the number of hash functions applied. Each  $h_j$  is a hash function that maps a 8-gram to a unique integer. This MinHash signature enables the AS to recognize similar applications based on kernel sequences without access to the actual kernel names.

**Aggregation Server Role.** The primary task of the AS is to check new snippet hashes against the EST to determine if they represent new or existing canonical snippets. If a snippet does not match an existing entry, the AS employs Jaccard similarity matching of the min-hashes, to compare the snippet

against all entries in the SST. This process identifies or assigns a canonical snippet, ensuring that similar sequences are grouped appropriately (small changes in kernel sequence arise as a result of input-dependent behavior which we want to capture). Jaccard similarity measures the similarity between two sets by dividing the size of their intersection by the size of their union, and it is commonly used in conjunction with min-hashes to efficiently estimate this similarity.

Jaccard similarity  $J(M_i, M_j)$  between two Min-Hash signatures  $M_i$  and  $M_j$  of two snippet sequences  $\mathbf{K}_i$  and  $\mathbf{K}_j$  is defined as:

$$J(M_i, M_j) = \frac{|M_i \cap M_j|}{|M_i \cup M_j|}.$$

If  $J(M_i, M_j)$  exceeds a pre-defined threshold  $\tau$ , then  $\mathbf{K}_i$  and  $\mathbf{K}_j$  are considered to represent the same application. We use  $\tau = 0.85$ .

### 3.2 Data Collection Phase

**Client role: Sampling Strategy.** Penrose employs a strategic sampling method to ensure comprehensive coverage across various applications and user environments. To achieve this, in the context of NCU for NVIDIA GPUs, we utilize a sampling technique where every  $N$ th kernel instance is selected after an initial offset, which is periodically adjusted to randomize the sample distribution. This method ensures statistical coverage of different kernel instances across multiple application runs and users. Additionally, the counter collected is rotated periodically to cover various hardware metrics. To keep slowdowns to a minimum, Penrose only supports metrics that can be collected without needing replays by NCU: this includes 51 metrics such as DRAM and SIMT utilization, L1/L2 cache misses for the A100. What pairs of counters avoid replays is hardware dependent — for the A100, we find of the 1275 possible pairings, a majority of them can be extracted with one pass. Collecting pairs of counters allows studying correlations within a kernel.

**Statistical Justification of Kernel Sampling Coverage.** Let an application execute  $k$  kernels per run. Each user samples one kernel every

$N$  executions, with the starting offset drawn uniformly at random from  $[0, N-1]$ . Over  $u$  independent users or runs, the probability that a specific kernel instance at index  $i$  is not sampled in a single run is:  $P_{\text{miss}} = 1 - \frac{1}{N}$ . The probability that it is *never* sampled over  $u$  runs is:  $P_{\text{never}} = (1 - \frac{1}{N})^u$ . Thus, the probability that kernel  $i$  is sampled at least once across  $u$  independent users is:  $P_{\text{hit}} = 1 - (1 - \frac{1}{N})^u$ . For example, with  $N = 100$  and  $u = 1000$  users, we have:  $P_{\text{hit}} \approx 1 - e^{-10} \approx 1 - 4.5 \times 10^{-5}$ , showing that nearly all kernel instances will be covered with high probability. This analysis holds for any deterministic or nondeterministic kernel sequence and generalizes to workloads with variable-length runs.

In Section 5.3, we empirically validate this behavior, showing that Penrose achieves over 99% application coverage in under 24 hours. The convergence behavior closely tracks the statistical guarantees derived here, confirming that Penrose’s lightweight sampling approach is both theoretically sound and practically effective.

**Client role: Data Aggregation.** To manage the volume of data efficiently and reduce transmission overhead, Penrose aggregates measurements into histograms at the user level. Specifically, we utilize 128-bin histograms for each collected metric. This is called the Partial Snippet Histogram (PSH), which aggregates all kernel measurements within a snippet into a single histogram on the user. When pairs of performance counters are collected, we need to decide how to produce a histogram of two variables. We observe that we can re-purpose our 128 bin histograms as a 2D 32x32 histogram, trading off fidelity of a single counter’s distribution for correlative information with a second counter. In this fashion, all the same feeds and speeds apply for the AS — we can simply aggregate these 32x32 histograms the same way as a single 128-bin histogram.

A PSH for an application is a histogram  $H_i = \{c_1, c_2, \dots, c_{128}\}$  of performance counters. Each counter value falls into one of 128 predefined bins (a system-level parameter decided by the DS). The value added to the bin is the number of kernels in that sampling interval for which that bin’s value was observed for that counter. Alternatively, the execu-

tion time of the kernel can be scaled (clipped) and discretized into a 4-bit number, ranging of 0 to 15, and we add this to the bin’s value. This discretization keeps all our arithmetic to integer data-types. This histogram is then encrypted using Paillier encryption before transmission. When the histogram reaches the aggregation threshold or exceeds a time-out, it is encrypted using an Additive Homomorphic Encryption (AHE) scheme and transmitted to the AS, accompanied by the snippet hash and snippet sequence minhash. Since we only need to perform aggregations, a fully homomorphic encryption system is not necessary for us. Specifically, we use Paillier encryption scheme [59, 38] with a 2048-bit modulus which provides fast additions over encrypted data (more details in § 3.3). Due to Paillier based encryption, the 8KB of plaintext data — 128 64-bit integers — expands to 32KB.

**Aggregation Server Operations.** Upon receiving a partial histogram of a snippet, the AS integrates these with an aggregated snippet histogram (ASH) using a additive homomorphic encryption (AHE) scheme.

**Designer Server Interaction.** The designer server periodically (as we will show shortly, the system achieves full coverage in 8 hours or so) retrieves updated histograms from the AS, specifically ASHs (which are encrypted), for further analytics. The decryption of this data is carried out using its secret key.

**Extensions.** Penrose has been designed with chip designers receiving the telemetry. It can be deployed and used by others like hyperscalars or data-center operators. Another extension is to use Penrose to aggregate differently: per-kernel histograms aggregated across all users. The DS can further log data internally as part of their telemetry pipeline to perform analytics on time varying behavior etc. Finally, the DS might desire data from different chip SKUs aggregated differently, whose trivial implementation is to dedicate an AS per SKU, or have the AS listen on different ports for each chip SKU.

### 3.3 Protecting User Privacy

As Penrose handles sensitive information related to user applications and their execution profile. We described the security and privacy requirements in § 2.3. Penrose meets those requirements with careful design choices as we describe next. In brief, **histogram confidentiality** is achieved with additive homomorphic Paillier encryption, allowing the AS to compute aggregate analytics, without learning the histograms of the performance data. This, along with Tor circuits to send updates, maintains **user anonymity**. **Application confidentiality** is protected via Hashing of sequence of kernel names (with optional name obfuscation at compile time).

We use Additive Homomorphic Encryption (AHE)—specifically schemes like Paillier—and Tor circuits instead of alternatives like Differential Privacy (DP) or Fully Homomorphic Encryption (FHE), due to better tradeoffs in privacy, utility, and efficiency in our context. AHE enables efficient summation on encrypted data without exposing plaintext, which aligns with Penrose’s goal of computing aggregate statistics. FHE, which supports arbitrary computation over encrypted data, is unnecessary since the Aggregation Server (AS) performs only summation. Various forms of Differential privacy (DP), such as LDP [27] and shuffle-DP [84], provides robust guarantees, particularly the ability to prevent reconstruction attacks, membership inference, and other forms of adversarial analysis through formalized privacy budgets. However, it could introduce significant noise —especially problematic in our setting where performance counter distributions are unknown. Our experiments showed that noise added by a DP mechanism degrades utility. Instead, in our system, the use of Tor ensures strong anonymity by decoupling data from identifiable users (this step can be thought of as the shuffle step in the shuffle-DP), and end-to-end encryption protects the data throughout its life cycle. Furthermore, our data consists exclusively of streams of integers without any associated metadata, auxiliary columns, or relational tables that could be exploited for attacks that exploit correlation of columns across multiple

tables [53, 32]. Thus, while we recognize the value of DP in certain contexts, it is not directly applicable to or necessary for our specific design. Penrose ensures privacy by encrypting partial histograms using AHE and transmitting them over distinct Tor circuits. As a result, the AS learns neither user identifiers (e.g., IP addresses) nor pseudo-identifiers (e.g., raw histograms). The DS only receives aggregated histograms and salted snippet hashes, with no linkage to individual users.

**1. User anonymity.** In Penrose, the Aggregation Server (AS) receives the following from participating users: an IP address, `PerfCounterId`, `SnippetHash`, `SnippetSeqMinHash`, and `Histogram`. The IP address is a direct identifier, while fields like `SnippetHash` or unique histogram patterns may act as pseudo-identifiers, potentially allowing AS to link updates from the same user.

To ensure user anonymity, Penrose implements the following safeguards: (a) Users’ IP addresses are hidden by routing updates through anonymity networks such as Tor [25], Mixnet [14], Loopix [61], or Apple’s iCloud Private Relay [66, 36]. (b) AS cannot view the contents of partial histograms due to the use of additive homomorphic encryption (AHE). (c) Each update message contains only one snippet hash and is sent over a distinct Tor circuits.

Public application snippet hashes are likely to appear across many users, making them unsuitable as unique identifiers. AS may learn how frequently a public application is executed in the wild, which is permissible under our threat model. In contrast, a private application’s snippet hash — likely associated with a single user — could act as a unique identifier. However, this only reveals the frequency of that application’s execution to AS, without linking it to the user’s identity, which aligns with our stated goals in § 2.3.

We experiment with Tor as it is widely used and vetted for privacy guarantees they provide.<sup>2</sup> In § 5, we demonstrate that the bandwidth requirement

<sup>2</sup>Tor might be vulnerable to Sybil attacks [46], that can violate the anonymity of end users. However, solving Sybil attack requires different set of techniques that is orthogonal to the goal of this paper, and Tor already has a number of mechanisms to reduce the risk of such attacks [46].

for Penrose is small (2MB/sec across 100,000 GPU nodes) and can be handled easily by existing Tor networks. To prevent the AS from tracking user behavior across messages, we set up a new Tor circuit for each communication to the AS.

**Summary:** *User anonymity is preserved.*

**2. Application confidentiality.** We want to ensure that AS or DS cannot learn the sequence of kernels of a private application a user is running. We consider the applications private for which AS or DS do not have access to the code or binary executable. For public applications, AS can learn the snippet sequence from the code or application binaries even without any update from the user. AS can use tools like `nsys` and other NSIGHT tools [19] to obtain a trace of kernels and use our public Penrose code to compute the snippet min-hash. Thus, we do not aim to protect the kernel sequence of public applications.

Thus, Penrose never sends the raw snippet — sequence of kernel names — to AS. Instead, Penrose sends snippet hash and snippet min-hash values computed using a secure cryptographic hash function such as SHA-256. From the snippet min-hash, AS learns the smallest hash value among all  $n$ -grams of kernel sequence for each hash function  $h_1, h_2, \dots, h_H$ . As Penrose uses cryptographic hash functions, these the only way to uncover the underlying  $n$ -gram from the hash values via *guess-and-check* approach used in password cracking [35, 47]. We show next that using such techniques are infeasible in our context due to modest alphabet size (number of unique GPU kernel names) and  $n$ -gram sizes we use,  $n = 8$ .

There are approximately  $N = 10^4$  publicly available NVIDIA GPU kernels [56]. Thus there are  $N^n$  unique kernel  $n$ -grams are possible. To uncover a hash value, AS has to bruteforce search in this large search space  $N^n$  kernel  $n$ -grams. We select  $n = 8$  to make this computation significantly harder; and for  $N = 10^4$ , we have  $N^8 \approx 10^{32}$ . The complete Bitcoin networks can compute about  $10^{21}$  hashes per second [77]. That means to break the hash value of an 8-gram, an adversary even with the compute power equivalent of the complete Bitcoin network in the world will take over 3,100 years. Although it is computationally hard to identify *any* kernel 8-gram,

an attacker could identify a set of popular 8-grams and learn their presence in an application.

To avoid such kernel  $n$ -gram identification, we propose to include a **per-application salt** selected by the *developer* during the application (or library) compilation for all users of that application (or library).<sup>3</sup> This can be done by GPU companies providing this as a compiler option (with developers concerned about application anonymity deploying their applications with this flag used during compilation). Or it can be done with a trivial source-to-source compiler that inserts a wrapper function name with an obfuscated name. For cases where the GPU chip company ships libraries in pre-compiled form, the developer can use a binary rewriter that mangles kernel names of these libraries before deployment. The telemetry capability we add needs to retain this kernel name anonymity. Our name mangling solution described above achieves this.

**Summary:** *The AS or DS does not learn anything about kernel names of private applications.*

**3. Histogram confidentiality.** Penrose ensures that AS cannot learn anything about the histograms performance counter (that they do not already know, like the number of buckets in each histogram, the number of performance counters in the telemetry data, etc.). To achieve this, we use an additive homomorphic encryption (AHE) [59] to encrypt the partial histograms so that AS cannot learn anything about the partial histograms but is able to compute the aggregation (summation over each histogram bucket). We use the Paillier’s AHE scheme [59].

DS selects a public-private Pailler key pairs during the setup of Penrose; DS publicly post the public keys (with certificates) on their website, from where users can download when they opt into Penrose. All users use the same public key. Paillier encryption of a message  $c_i$  — a histogram value in our case — with a public key  $pk = (g, n)$  is defined as follows:  $\text{Enc}_{pk}(c_i) = g^{c_i} \cdot r^n \pmod{n^2}$ , where  $r$  is a random number selected per encryption. After receiving encrypted histograms, the AS can aggregate them without decryption using Paillier’s homomorphic prop-

erty:  $\text{Enc}_{pk}(c_1) \cdot \text{Enc}_{pk}(c_2) = (g^{c_1} \cdot r_1^n \pmod{n^2}) \cdot (g^{c_2} \cdot r_2^n \pmod{n^2}) = (g^{c_1+c_2} \cdot (r_1 \cdot r_2)^n \pmod{n^2}) = \text{Enc}_{pk}(c_1 + c_2)$ . Thus, AS can simply multiply the encrypted values in each histogram bucket from different updates for the same snippet hash for the same performance counter to create the ciphertext of the sum of the underlying histogram values. Only DS who has the private key can decrypt these ciphertexts. When DS receives the encrypted aggregated histograms, they decrypt the aggregate ciphertexts to obtain the aggregate snippet histogram, but cannot learn about the partial histograms.

In our implementation, we use a public key size of 2048-bits, which can encode any 64-bits value and operate on it without the worry of any overflow even after trillions of additions. NIST recommend 2048-bit keys (Table 2 in [6]) as provide sufficient security (equivalent of 112-bits) for most applications.

**Summary:** *Data confidentiality is preserved - the DS sees only aggregated histograms, with the AS obtaining no visibility to data.*

**Additional privacy considerations/Extensions.** In our threat model we considered all parties to be honest but curious. Malicious users could submit fake partial histogram data to AS to subvert the accuracy of the analytics system (i.e. these poisoning attacks are well known in ML [78] and techniques to combat these attacks can be readily layered on top of Penrose). One approach for handling poisoning is that the client proves using ZKPs that the data under encryption satisfies a validity predicate (called input validation), such as Eiffel and ACORN [16, 1]. However, these solutions incur too much overhead in our context. Hardware attestation like the one available in the latest generation of data-center class GPUs like Hopper could also be used to verify the veracity of the partial histograms. H-100 GPUs provide device identity certificate signed with a device-unique ECC-384 key pair [5] and can sign the performance counters that can be verified that the data is indeed generated on a legitimate GPU. Other similar techniques such as anonymous attestation [10, 11, 13] or enhanced privacy ID (EIPD) introduced by Intel [39, 12] could be used as well. Moreover several prior works provide approaches to transform semi-honest protocols to a

---

<sup>3</sup>At present CUDA compiler, as far as we know, does not allow the CUDA kernel name to be stripped or obfuscated.

protocol that is secure in the fully malicious model (see [41] and [9]) can be applied to Penrose as a mitigation, with some optimizations needed to reduce their overheads.

### 3.4 Discussion

**Handling of Distributed and Multi-GPU Workloads** Penrose naturally supports multi-GPU workloads by analyzing each GPU’s execution timeline independently. In distributed ML inference, where techniques like tensor parallelism result in many short-lived kernels, Penrose continues to operate effectively by sampling and classifying kernel sequences on each participating GPU. These sequences are then aggregated using the same privacy-preserving mechanisms across users. Synchronization across GPUs does not hinder Penrose, since telemetry is local to each GPU and privacy aggregation happens post hoc. While our prototype does not yet coalesce cross-GPU snippets into a unified graph, the core profiling and aggregation mechanisms remain valid and scalable in distributed inference and training contexts. Future work could enhance snippet alignment across GPUs to better model full workflow topologies. Importantly, such cross-GPU correlation is a post-processing engineering task and orthogonal to the scientific contribution of Penrose, which is the secure, scalable aggregation of local telemetry. Additionally, our measured workloads already include many kernels with durations significantly shorter than typical ML inference kernels—placing Penrose under even more challenging conditions. Thus, the system has been empirically validated in settings stricter than those posed by distributed inference workloads.

## 4 Evaluation Methodology

**Penrose system simulator.** To evaluate Penrose, we built a system-level event-driven simulator that models  $G$  GPUs, the aggregation server (AS), and the designer server (DS). The simulator models the network traffic between GPUs, AS and DS. The computation on the user-side (kernel execution and

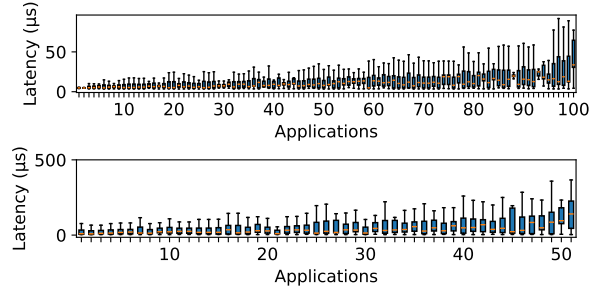


Figure 4: Latencies of kernels per application for 154 applications we tested. Three applications whose maximum kernel latencies exceeded  $500\mu\text{s}$  are not shown here. X-axis is application number, with the “small” 100 shown in the 1st plot.

data-encryption), and AS is modeled as atomic tasks and blocking computation. Specifically, the GPU model comprises of sampling the kernels at the provided sampling interval, and sending a message to the AS. On the AS, when a message is received an aggregation computation task is kicked off. The simulator models different sampling rates, and implements offset switching at a given sampling reset interval ( $O$ ). It also implements a load factor which models a user being active or inactive at any given time interval. E.g., if a  $O$  is 600 seconds and the load factor is 10%, then the simulated GPU will only sample kernels for 60 seconds for that interval. The output of this simulator is both functional behavior (producing aggregated snippet and kernel histograms) and performance (producing the execution time needed to achieve coverage, and network traffic sustained at different system parameters). Penrose’s planet-scale behavior modeling is necessary for demonstrating coverage.

**Applications.** We feed kernel traces obtained from 154 Torchbench applications comprising of inference and training applications [34, 49] to the simulator. The kernel trace is obtained by running each application on an NVIDIA A100 GPU using Nsight Systems (NSYS) to obtain the execution time of each kernel which is used for GPU node simulation. The recorded execution time of kernels for each applications is shown as a box-plot in Figure 4. Kernel la-

tency vary between 3s to 521s, at an average of  $30\mu s$ . The number of kernels executed for one batch of samples (batched inference or a training mini-batch) ranges from 14 to 128,838, with a median of 870.

**Measurements from prototype.** Our simulator is augmented with measurements from our prototype of Penrose’s critical components. These include an AHE histogram aggregation implemented with Intel’s Paillier library. Our min-hash similarity algorithm is implemented in Python and is already fast enough (taking 11 milliseconds to match against 2000 applications; lookups in a 128K entry EST takes  $0.6\mu s$ ). Finally, we separately ran all of the benchmarks with Nsight Compute (NCU) natively on a single A100 GPU for our user experience experiment. We obtain slowdowns from sampling by running with sampling rates of 1/1000, and 1/10000. We used CloudLab to run a scaled representation of Penrose traffic through Tor (reducing the number of nodes by  $\sim 3000\times$  but increasing the traffic rate by  $\sim 3000\times$  to compensate).

**Simulator Validation.** Our in-house event-driven simulator is tightly grounded in a real deployment on CloudLab. Specifically, we implemented the full Penrose stack, including a socket-based aggregation server (AS) running on a Xeon-class m3.small.x86-like instance and 100,000 concurrent client processes simulating telemetry upload (100 real physical clients at 1/100 sampling). This deployment faithfully captures the communication overheads in Penrose, including additive homomorphic encryption, socket I/O, and periodic histogram updates. While we cannot practically run 100,000 real GPU clients, we emulate this scale using randomized inputs and validate the simulator against the runtime behavior of our prototype. The simulator is used exclusively for projecting long-run convergence times over hours of global telemetry. By design, Penrose makes the server code fast.

## 5 Evaluation

We now evaluate the effectiveness of Penrose to understand whether it can be effective and its costs of deployment. Penrose has a complex design space

with many potential parameters and policies that can be tuned to adhere to bandwidth / compute constraints of real-world systems. Because of this complexity, we select a canonical value for each parameter listed in Table 1. We primarily evaluate the feasibility of our system design for this set of parameters on Torchbench, while performing some design space explorations along particular dimensions of our design.

To clarify the scope of our evaluation, we explicitly distinguish between results derived from real measurements and those obtained via simulation. All measurements related to GPU application profiling, encryption overhead, application coverage accuracy, slowdown characterization, and histogram aggregation performance are based on real experiments conducted on NVIDIA A100 GPUs and standard CPU servers. Specifically, Figure 4 (kernel execution latency distribution), Figure 5 (sampling slowdown), Table 2 (snippet identification accuracy), Table 3 (encryption and aggregation throughput), and Figure 7 (performance counter state breakdown) are all based on measured data. Only the large-scale convergence experiments in Section 5.3—namely, the time to achieve statistical application coverage when scaling to tens or hundreds of thousands of GPUs—are based on our discrete event simulator.

### 5.1 Guiding Questions

1. What is end-to-end application slowdown due to Penrose?
2. Can Penrose achieve coverage of applications and performance counters within a reasonable amount of time?
3. What is the overhead of using AHE with Penrose?
4. Overall, what is the cost of our system and is it cost-effective?

### 5.2 Q1: Measuring User Slowdown

Reading GPU performance counters using NCU introduces slowdowns, which we mitigate by sampling every  $S^{th}$  kernel. We study the effectiveness of this

Var.	Description	Default	Units
$L$	Snippet length	10,000	Kerns
$S$	Sampling interval	10,000	Kerns
$O$	Sampling reset interval	600	Seconds
$A$	Aggregation threshold	10,000	Samples
$\delta$	Server report interval	1	day
$G$	Users per server	100,000	GPUs / Server

Table 1: Different parameters used by Penrose.

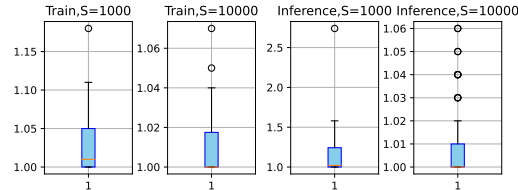


Figure 5: Application slowdown from ncu for Torchbench for 1/1000 and 1/10,000 sampling for Train and Inference.

mitigation by measuring the *application level slowdown* incurred by different sampling intervals. Figure 5 shows a box plot of application slowdown for *sampling intervals* of 1000 and 10000. For  $S = 1000$ , we observe an average slowdown of 7.55% across training and inference tasks, excluding outliers, and a maximum slowdown of 174% (a very short application for which NCU’s book-keeping overheads was dominating). For  $S = 10,000$ , we observe an average slowdown of only 0.045% across training and inference, with a maximum slowdown of 7%. Based on this experiment, we choose  $S = 10,000$  as a practical configuration.

**Takeaway:** *Penrose is effective at mitigating user slowdown with sampling, resulting in an average slowdown of 0.045% across 154 real-world DL applications.*

### 5.3 Q2a: Application Coverage

Sampling kernels for performance monitoring introduces a new problem: how to ensure that performance data of all kernels are considered in the aggregated histogram to accurately represent application-

level performance. We define “full” coverage for an application as having recorded data for a performance counter for all of its kernels. Coverage for one application, then, is expressed as a fraction of kernels whose data has been reported to the AS. If we run 154 applications on 100,000 GPUs, we get full coverage in a few minutes. Across Torchbench, average kernel execution time is only  $30\mu s$ , and with an uniform distribution every application has 600 copies running simultaneously. For this experiment, we instead simulate 2000 unique applications built from this list of 154 — each application has 13 copies, each of which is treated as a unique application. We also take this application set of 2000 and create two normal distributions, In **normal-large**, the applications with the longest number of kernels are most frequently executed by users. In **normal-small**, the applications with the fewest number of kernels are most frequently executed by users. In both cases, the distribution has a mean of 1000 and std-deviation of 333. This implies that with **normal-large**, 11.9% of the applications are the top-200 largest, 38% of the applications are the largest 660 applications, and 68% are the largest 1320 applying standard probability calculations. Real world application mix will fall in-between these two normal distributions. Figure 6 shows the *average* application coverage of both 1000 and 2000 applications as a function of time (hours) to demonstrate how coverage improves as the ratio of users to applications increases in all 3 cases. We can see that for our canonical scenario, we easily achieve  $> 99\%$  coverage in 8 to 24 hours. If a designer was interested in 10 performance counters, they could chose to wait 10 days for  $> 99\%$  coverage, or get 85% of the

# APPS	100,000 GPUs			10,000 GPUs		
	U	$N_s$	$N_l$	U	$N_s$	$N_l$
2000	2.3	13.5	9.5	15.3	14.5	12.7
1500	2.3	11.8	7.5	13.7	16.7	9.2
1000	1.5	10.5	4.8	10.2	13.2	8.8
500	0.7	5.2	2.3	6.7	15.2	10.2
200	0.2	2.3	1.0	2.2	11.3	11.7

Table 2: Hours to cover 97.5% of apps.

applications  $\times 10$  counters covered every day by controlling when they switch which performance counters are sampled. We also report the amount of time each application took to reach  $> 99\%$  coverage in the scatter plot. The green lines show the time taken for 97.5% of the applications (1950 of 2000) to reach  $> 99\%$  coverage.

We studied and simulated systems of different scale (10,000 GPUs to 1 million GPUs), while keeping  $S$  constant. With a million GPUs, Penrose achieves effectively the same coverage trends with 20,000 applications. The curves are indistinguishable on the graph.

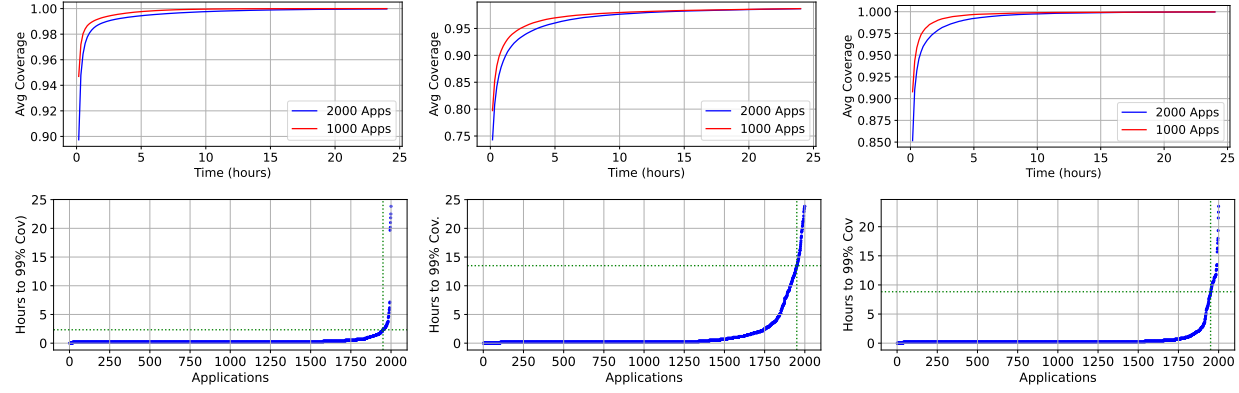
**Takeaway:** *Based on our simulation, we find that high coverage is easily achieved when the number of participants ( $G$ ) is large even with seemingly low sampling rate of  $S = 10,000$ . Across a deployment of 100,000 GPUs, we find the system can still achieve  $> 99\%$  coverage in a day even when there are up to 2000 popular applications running in the wild, scaling to 20,000 applications with 1 million GPUs.*

Table 2 examines time-to-coverage under different deployment scales and application distributions. We vary the number of GPUs (from 100,000 to 10,000) and the number of distinct applications (from 2000 to 200), across three distribution models: UNIFORM ( $U$  (apps appear with equal probability),  $N_s$  (apps with few kernels dominate), and  $N_l$  (apps with many kernels dominate)). We report the time (in hours) required to achieve 99% snippet coverage for 97.5% of applications. As expected, fewer GPUs increase time to convergence, but the impact is modest: even with a 10 $\times$  reduction in GPUs, time increases by only  $\sim 2\text{--}3\times$ . Distribution shape also influences convergence—skewed workloads dominated by small kernels

( $N_s$ ) take significantly longer to cover; since the apps with many kernels appear infrequently. As we decrease the number of applications, convergence happens faster. These results confirm Penrose remains effective across varying deployment sizes and workload skews.

**Measurements:** To address concerns about relying on simulation and to validate our approach on physical hardware, we deployed Penrose on a 32-node A100 GPU testbed within our internal cluster. In this deployment, we developed a wrapper script to select  $N$  applications from the Torchbench suite. Each GPU repeatedly executed its assigned application. The applications were profiled using ‘ncu’ with a sampling rate of 1/10000. We conducted 7 cohorts of experiments, varying the number of concurrent applications ( $*N^*$ ) from 1 to 32 in powers of two. For each cohort, we ran up to 30 trials, with each trial selecting a random set of  $N$  applications; for the 1 application setting we ran 154 trials. To ensure a diverse mix, one-third of the trials for each cohort used a normal-small distribution for application selection, one-third used a normal-large distribution, and the final third used a uniform distribution. In total, we executed 382 distinct experiments over approximately 20 days, accumulating 470 hours of total GPU execution time. The longest experiment (32 apps) ran for 21 hours.

Figure 7 presents a box plot illustrating the time to achieve convergence 97.5% for these experiments as the number of applications is varied. As one might expect, at a low number of applications, there is considerable variance in convergence time, depending on whether a small or large application was chosen. At a scale of 8 to 64 applications, the system consistently achieved full coverage within 4 to 12 hours. Most importantly, this large-scale experiment demonstrates Penrose’s capability to collect data effectively on real hardware. To validate our simulator, each of these hardware application mixes was executed within our discrete-event simulator. The simulator produced convergence times identical to the hardware measurements. While a perfect match might seem surprising from the perspective of traditional cycle-level simulation, it is the expected outcome for our system’s level of abstraction. This deterministic result occurs because both the physical deployment and the sim-



(left) Uniform distribution (middle) Normal Dist (small apps most frequent) (right) Normal Dist (large apps most frequent)

Figure 6: Average coverage (1000 and 2000 apps) and Time to 99% coverage (2000 apps) averaged across all simulated applications for 100,000 GPUs. The green vertical line marks the 97.5%-th percentile (1950 applications). Load factor is 10% for all scenarios.

ulation are driven by the same sequence of discrete events: intermittent messages sent from each GPU to the aggregation server. With a sampling interval of 10,000 seconds and aggregation of 10,000 samples, the worst case is a message every 530 seconds for the application `soft_critic` which has avg kernel execution time of  $5.3\mu\text{s}$ . Any real-world timing “jitter” in message arrivals—on the order of milliseconds or seconds—is orders of magnitude smaller than our final measurement granularity, which is in 100s of seconds. The encryption time which the simulator doesn’t account for is measured on the order of 100ms to 400ms. The simulation, therefore, correctly models the exact sequence of events that dictates convergence, leading to an identical result. It is important to note that as the system scales to thousands of GPUs, the primary challenge becomes managing network effects on the server, which we discuss later in this section. The load on individual clients, however, remains constant regardless of system size.

Of course. This is indeed a very strong result, and presenting it clearly will be highly effective. The key is to guide the reader from the experimental setup to the main takeaway in a logical, data-driven narrative.

Here is a refined version of the paragraph that aims for better flow, clarity, and impact, suitable for a

research paper.

\*\*\*

A crucial aspect of our methodology is quantifying the measurement error introduced by sampling. To this end, we conducted a rigorous validation experiment. First, we established a ground truth by generating “perfect” histograms of DRAM memory bandwidth for 154 applications, running each on a single GPU to capture its complete execution profile. We then generated corresponding sampled profiles by running each application across 32 GPUs, collecting data at a 1/10000 sampling rate, and aggregating the results. By comparing the sampled histogram to the ground truth for each of the 128 bins per application, we computed the relative error across a total of 19,712 data points.

Figure 8 visualizes the results as a scatter plot, with the fractional execution time represented by a bin on the x-axis and the corresponding relative error on the y-axis (note both axes are on a log scale). The plot clearly demonstrates that Penrose is extremely accurate. The average relative error across all bins and all applications is a mere 1.12

More importantly, the figure reveals a critical trend: the largest errors occur only in bins that account for a negligible fraction of the application’s to-

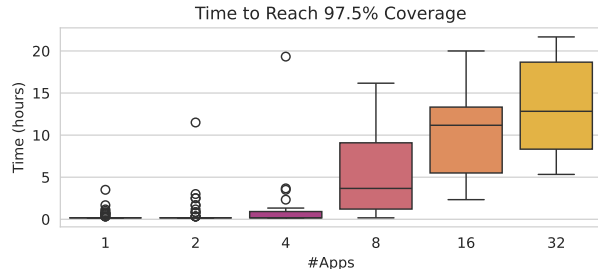


Figure 7: Time for convergence on GPUs. Small experiment.

L	Snippet (%)	App (%)
500	79.96	77.27
1000	90.40	87.66
5000	95.36	95.45
10000	95.36	95.45
20000	95.36	96.10

Table 3: Snippet and app identification accuracy across ( $L$ ).

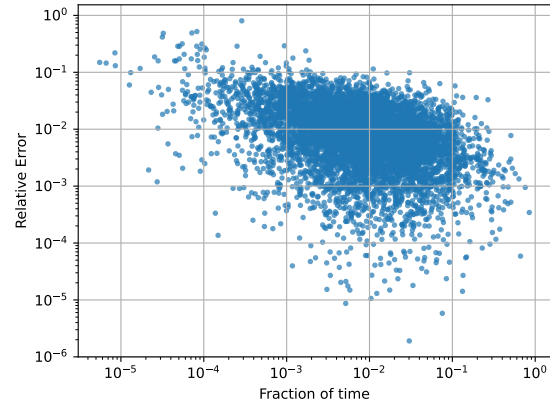


Figure 8: Relative errors in histograms.

tal execution time. Across the entire dataset, only 276 of the 19,712 bins (1.4%) exhibited an error greater than 5%, and the combined execution time represented by these infrequent bins amounts to just 0.064% of the total. This result is a direct consequence of the law of large numbers; any significant deviations from sampling are confined to infrequently executed kernels that contribute minimally to the overall performance profile. This experiment provides strong evidence that our sampling methodology is robust and accurately captures the performance characteristics that matter most.

#### 5.4 Q2b: Snippet Coverage

We now evaluate our snippet classification covering its accuracy, latency, and memory storage needs.

**Accuracy.** To measure accuracy of our snippet classification implementation, we generated 50 snippets per application, labeled the first snippet as the canonical snippet, and measured how the 49 other snippets were matched to that snippet or not. To generate these snippets, we take each application’s execution over a large number of epochs, providing a large sequence of kernels. Each snippet starts at a random location in this sequences and is  $L$  consecutive kernels. Table 3 shows the accuracy results for different sizes of the snippet length. All results are for 100 hash functions for the min-hash with the Jaccard similarity threshold set to 0.85. With 154 applications and 50 snippets per application, every snippet is matched against 154 canonical snippets — meaning we perform a total of  $154 * 50 * 154$  comparison. Any time a snippet matches closer to a snippet different from the canonical snippets that is a mismatch. The accuracy at this snippet level is shown in the 2nd column, which measures  $1 - \#mismatches / (154 * 50)$ . It is generally very high — since most snippets match correctly. Application level accuracy, narrows this down to how these mismatches are spread across application. At  $L \geq 5000$ , we see accuracy is greater than 95% meaning, snippets belonging to fewer than 7 applications among the 154 are ever misclassified. In all the mis-classifications, an application’s similarity to another application was equal to or greater than the match to the “correct” application. When snippet length is too short, it doesn’t sufficiently

cover the full behavior of an application leading to more mis-classifications.

**Storage.** On the aggregation server, we also maintain a cache of the min-hashes as an optimization to avoid doing the similarity every time a snippet reaches the AS (matching a snippet against 154 canonical matches takes  $< 1$  ms). We observe for 2000 applications, with a snippet length of 10,000 and 32B hashes, a server-side snippet table would only grow to be  $2000 \times L \times 32B = 610.35MB$  in size – easily held in memory on modern servers with terabytes of RAM.

**Takeaway:** *Based on our simulation, we find that our snippet lookup system, when  $L = 10,000$ , is both fast and accurate, while taking up a small amount of space. Therefore, it is feasible that Penrose would quickly construct robust snippet tables.*

## 5.5 Q2c. Practical Counter coverage

How many and what counters can be serviced by Penrose is hardware dependent — the key requirement being that the counter must be obtainable without replays to mitigate application slowdowns. In addition, we can capture pairs of counters that can be measured without replays. On the A100, there are 51 metrics such as DRAM and SIMT utilization, L1/L2 cache misses, among approximately 100 others that can be supported, and about half of all the pairwise combinations of these counters<sup>4</sup>. Since we build partial histograms, to understand the interplay between multiple performance metrics for a given application we need such simultaneous measurement which Penrose provides. As a motivating example of such analysis, Figure 9 shows a runtime breakdown for BERT, DALLE2, Learning to Paint(LtoP), and Alexnet (Anet), across both training and evaluation, into four states based on the utilization of DRAM and TensorCores: both low ( $\leq 33\%$  of peak), one of tensor or DRAM low, or neither low. This breakdown allows us to understand more deeply the performance characteristics of an application. Data for all applications omitted here for space reasons, released with paper.

<sup>4</sup>In the interest of space, we omit the full list.

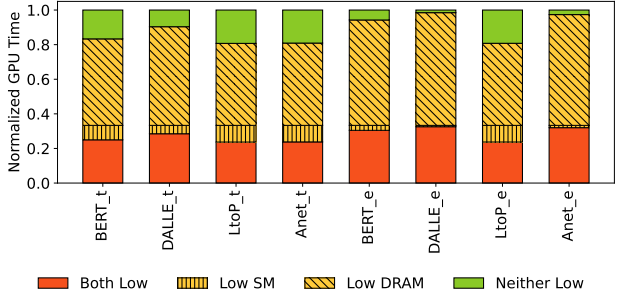


Figure 9: TorchBench time spent in different combinations of Tensor and DRAM utilization attainable using Penrose. First 4 bars are Training; next 4 are inference.

This reveals a previously undocumented pattern in real-world GPU workloads: execution phases often underutilize either Tensor Cores or DRAM bandwidth, but rarely both simultaneously. This decoupled behavior suggests a systemic inefficiency in overlapping compute- and memory-bound operations. Unlike prior work such as Splitwise, which emphasizes sustained bandwidth saturation, our results indicate that substantial slack remains in overlapping disjoint pipeline stages. This opens up new avenues for architectural optimizations—such as fine-grained kernel fusion, prefetch scheduling, or smarter warp dispatch—to increase concurrent utilization of GPU subsystems. These findings were only made possible through Penrose’s ability to collect fine-grained, large-scale telemetry across a diverse application population, and they serve as an example of the insights such a system can uncover.

**Takeaway:** *Penrose is capable of extracting out combination states of supported hardware metrics as efficiently as a single metric.*

## 5.6 Q3: Overhead of AHE and User Anonymity

General computation with **FHE** has  $1000\times$  to  $10000\times$  overheads, and introduces further issues of noise and bootstrapping when many operations are performed. However, through careful design, Pen-

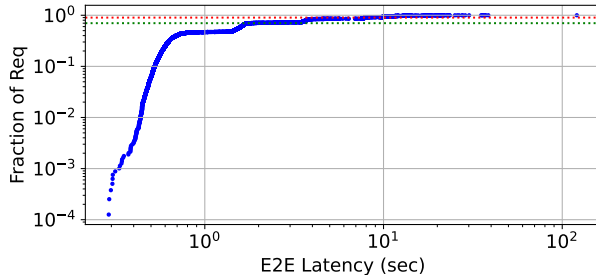


Figure 10: End-to-End Latency (log-log plot) Through Tor from Clients to AS. Green indicates 70% of requests, red 90%.

rose only needs addition operators and hence we use the Paillier crypto system which allows addition operations on encrypted data. The key implementation issue is data-size growth and speed. As mentioned in the security section we use a modulus of 2048 which allows RSA 112-bit security. With this modulus, the data growth is  $32X$ , meaning each of our 128-bin histograms of 64-bit ints (which is 1KB in plaintext) is 32KB in ciphertext. In terms of speed, we are concerned about **encryption speed** at the clients (their partial histograms need to be encrypted before sending to the AS), **aggregation speed** at the AS, and **decryption speed** at the designer server. Recall that the AS needs to aggregate requests across all GPUs (100,000 in our default case). Clients need to perform an encryption of a partial histogram every 3000 seconds (*average kernel time*  $\times A$ ).

Table 4 summarizes these speeds. For client encryption speed we made our measurements on an “old” Ryzen laptop and a higher-end Intel Core i5-11500, restricting the computation to 1-core. These measurements indicate an overhead of 0.014% to 0.0035% since this is performed once every 3000 seconds. For the aggregation server we make measurements on a server class CPU (12-core Intel Xeon E-2378G) — it can sustain almost 10 $\times$  the needed computation throughput. The designer server’s application is light, with decryptions running fast. Recall the designer server request a full histogram once every 8 to 24 hours.

Looking at network transfer rates, every client generates traffic of 32KB every 3000 seconds. The AS

sees an aggregated incoming traffic across all of its GPUs of 0.12 GB/sec, well below a 25 Gbps link. At steady state, the Tor network would be responsible for this level of traffic which represents about 0.4% of Tor’s typical relay bandwidth [79]. We also measured Tor performance by measuring the end-to-end latency (open socket, connect to SOCKS proxy on client, send message, close socket upon ack) to deliver the data to the AS. We did this measurement on a scaled system with 32 nodes sending requests every 0.96 seconds (essentially with fewer nodes we send traffic at a proportionally rate faster. 10 $\times$  fewer nodes send data 10 $\times$  more frequently.  $0.96\text{sec} = 3000/(100000/32)$ ). We used 32 nodes on Cloudlab [18] running Tor, and instantiated the AS outside Cloudlab to send traffic to. We simulated 10 hours of traffic. Figure 10 shows distribution of the observed end-to-end latency to send the partial histograms to the AS. 70% of requests see a latency  $< 2$  seconds, 90% see latency  $< 8$  seconds, less than 5% of the requests see latency  $> 11$  seconds. For context, fetching the standard `curl --socks5 127.0.0.1:9050 https://api.ipify.org`; takes on average 0.85 seconds on Tor with high variability, sometimes taking 6 seconds. Through the entire duration, the server (which was a python prototype code) easily handled all messages.

Each client sends 32KB every 3000 seconds, resulting in an aggregate AS traffic of 0.12GB/sec—well below the 25Gbps limit. At scale, this would represent just 0.4% of Tor’s relay bandwidth [79]. To evaluate end-to-end Tor performance, we used 32 Cloudlab [18] nodes sending data every 0.96s (mimicking 100,000 GPUs by scaling up the per-node rate). The AS ran outside Cloudlab, and we simulated 10 hours of traffic. Figure 10 shows that 70% of requests had  $<2$ s latency, 90% had  $<8$ s, and  $<5\%$  exceeded 11s. For reference, a standard `curl` request via Tor averages 0.85s with spikes to 6s. The prototype server handled the full traffic load without issue.

**Takeaway:** *Based on our measurements, Penrose effectively uses computation on encrypted values without it becoming a computation bottleneck. Off-the-shelf servers are more than sufficient to meet the computation, memory, and network traffic needs.*

Client (Latency for 1 histogram)	
Enc Speed (AMD Ryzen 7 4700U)	431 ms
Enc Speed (Intel Core i5-11500)	105 ms
Aggregation Server Tput (Histogram Aggregated/sec)	
Intel Xeon E-2378G	8075
Required tput to serve 100,000 GPUs	33.3
Designer Server	
Decryption Speed (Intel Xeon E-2378G)	27 ms

Table 4: Speed measurements

### 5.7 Q4: Cost Effectiveness and System Balance

Answering the above questions provide limit studies on what is possible for choice of sample interval, possible coverage, and AHE effectiveness. This subsection ties together and balances multiple intersecting constraints: \$ cost of the server, number of GPUs one AS can serve, network, computation, and storage needs. Our prototypical AS choice would be a m3.small.x86 Equinix instance [26] with a 25 Gbps network link, 1 x Intel Xeon E-2378G, and 64GB memory. It has a Total Cost of Ownership (TCO) of \$5519 per year.

**Computation needs.** For each client, we defined the aggregation threshold to be  $A = 10,000$  samples. Assuming every kernel sampled is part of the same snippet, we expect each user to send out a new partial histogram every  $A \times S \times \text{Avg. Kern Lat} = 3000$  seconds. For  $G = 100k$  users, this means one AS receives  $100,000/3000 = 33.3$  partial histograms per second. Given our measured aggregation throughout of 8075 histograms per second, far in excess of this 33.3, implying HE computation overheads are not a bottleneck for the AS. Total data transfers into the AS is  $33.3 \times 32KB \text{ per message} \times 2$  which is well below 25 Gbps.

**Storage Growth Rate.** Histograms allow our system to reduce the storage needed for analytics data. Given a snippet table of 2000 apps and  $32KB$  ciphertexts, the maximum amount of storage needed per report period would be  $2000 \times 32KB = 64MB$ , which a modern server could easily accommodate.

**Correctness of encrypted computation.** A

subtle issue of correctness and overflow merits attention. Given a worst-case where each client pushes a partial histogram every 3000s, and our canonical parameters of  $G = 100k$ ,  $A = 10k$ , and  $\delta = 24$  hours, the maximum value an aggregated histogram bin could reach before being sent to the designer server is  $G \times A \times \delta/3000s = 1.887 \times 10^{15}$ . This falls within the 64-bit int range, and a 2048 bit modulus allows encrypted representation in Paillier crypto systems.

**Larger histograms.** Histogram size scales system costs linearly. For 1024 bins, the AS handles 1023 aggregations/sec—well above the 33/sec required. Network traffic remains modest at 0.016 GB/sec (vs. 25 Gbps link), and client-side encryption takes 3.3 seconds, amounting to just 0.11% overhead. Simple scheduling (e.g., `nice`) suffices to amortize this across the 3000-second window.

**Takeaway:** *Our design of the different parameters provides a cost effective and balanced solution, which can be scaled out to support more GPUs (in ratios of one aggregation server to 100K GPUs). The amortized system cost of Penrose is low: 6 cents per GPU per year.*

## 6 Related Work

**Industry solutions.** Nascent solutions include NVIDIA’s GeForce Telemetry [55] which collects some data on hardware and software configuration. Techniques like running profiling tools in-house by a chip designer or software developer, don’t provide in-the-wild behavior. Hyperscalars like Google [30], Meta [20], Amazon [3], Intel [37], and

Microsoft [50] have in-house telemetry solutions. 3rd party continuous profiling services include Datadog’s continuous profiling [23], Pyroscope [31], parca [73], ydata-profiling, [17], and Splunk’s AlwaysOn profiler [74]. The most relevant of these is Dynolog [20] — which integrates with the PyTorch profiler and Kineto CUDA profiling library. However, to the best of our knowledge and publicly disclosed it does not capture low-level GPU performance counters which introduces issues with slowdowns. Second, it assumed knowledge/control of the application — i.e. a chip designer (or pytorch model developer) would not be able to transparently get access to this information. These tools generally assume the entity doing the profiling has full control of the application either of a single-node or an entire cluster/data-center.

Industry systems like NVIDIA’s DCGM and Google-Wide Profiling offer valuable telemetry but differ fundamentally from Penrose. These solutions operate within a single administrative domain, require full control over the software stack, and provide no privacy guarantees. Penrose, by contrast, supports privacy-preserving telemetry across organizations where application binaries are opaque and workloads are user-deployed. Unlike prior work that assumes centralized control, Penrose identifies applications from encrypted kernel streams and aggregates performance data securely—enabling **chip designers** to gain insight from real-world deployments beyond the reach of existing tools. It complements, rather than replaces, internal telemetry stacks.

**Research profiling tools and frameworks.** Frameworks and methodologies for profiling in the data-center include Propellor [68], Accelerometer [75], and Dmon [43] — they don’t focus on GPUs or the type of in-the-wild low-level hardware counters including the application identification challenge we solve. Large-scale application characterization studies include [24, 80, 67, 42]. Continuous profiling was originally introduced in [4], and has since been used in a number of contexts. vprof and AutoCPA utilize continuous profiling to optimize source code [81, 64]. [65] implements a private continuous profiling framework for IoT-enabled networks. LightGuardian and OmniWindow propose a novel in-flight telemetry for

networks like we envision for compute [83, 76]. Basic block vectors were proposed as way for program characterization and later work expanded for automatically characterizing large scale program behavior and simulation strategies, bearing similarity to our snippet classification [69, 70, 45, 71, 33, 44, 72].

**Privacy.** Privacy-Preserving Machine Learning (PPML) encompasses secure training, inference, and federated learning [63, 82, 52]. Our focus is on computing a function  $f$  over private datasets, without revealing the data—specifically, via secure histogram aggregation. This is a simplified instance of broader secure aggregation problems [8]. Relevant applications of AHE and FHE include [28, 48, 62, 22, 54, 29].

## 7 Conclusion

As the complexity of both applications and hardware increases, GPU chip manufacturers face a significant question: how to gather comprehensive performance characteristics and value profiles from GPUs deployed in real-world scenarios? Such data, encompassing the types of kernels executed and the time spent in each, is crucial for optimizing chip design and enhancing application performance. This paper undertakes an ambitious system to provide extensive data in a privacy-preserving fashion combining ideas of sampling, data reduction through histograms, and AHE-based computation to preserve privacy. Our system Penrose shows that a single aggregation server matching a typical *small* compute instance cloud server can manage and collect profiles for 100,000 GPUs. At typical load rate of 10% activity and with 100,000 participating GPUs, Penrose achieves 99% coverage of applications in one day, thus being able to provide a type of streaming data of application behavior change.

## References

- [1] Acorn: input validation for secure aggregation. In *32nd USENIX Security Symposium (USENIX Security 23)*, 2023.

[2] Abbas Acar, Hidayet Aksu, A. Selcuk Uluagac, and Mauro Conti. A survey on homomorphic encryption schemes: Theory and implementation. *ACM Comput. Surv.*, 51(4), July 2018.

[3] Amazon. Codeguru. <https://aws.amazon.com/blogs/machine-learning/optimizing-application-performance-with-amazon-codeguru-profiler/>.

[4] Jennifer M Anderson, Lance M Berc, Jeffrey Dean, Sanjay Ghemawat, Monika R Henzinger, Shun-Tak A Leung, Richard L Sites, Mark T Vandeveno, Carl A Waldspurger, and William E Weihl. Continuous profiling: Where have all the cycles gone? *ACM Transactions on Computer Systems (TOCS)*, 15(4):357–390, 1997.

[5] Emily Apsey, Phil Rogers, Michael O’Connor, and Rob Nertney. Confidential computing on nvidia h100 gpus for secure and trustworthy ai. nvidia techblog <https://developer.nvidia.com/blog/confidential-computing-on-h100-gpus-for-secure-and-trustworthy-ai/>, 2023.

[6] Elaine Barker. NIST special publication 800-57 part 1 revision 5. recommendation for key management. <https://doi.org/10.6028/NIST.SP.800-57pt1r5>, 2020.

[7] A. Bhowmick, D. Boneh, S. Myers, K. Talwar, and K. Tarbe. The apple psi system, 2021.

[8] K. A. Bonawitz, Vladimir Ivanov, Ben Kreuter, Antonio Marcedone, H. Brendan McMahan, Sarvar Patel, Daniel Ramage, Aaron Segal, and Karn Seth. Practical secure aggregation for federated learning on user-held data. In *NeuRIPS Workshop on Private Multi-Party Machine Learning*, 2016.

[9] Dan Boneh and Victor Shoup. A graduate course in applied cryptography, 2023.

[10] Ernie Brickell, Jan Camenisch, and Liqun Chen. Direct anonymous attestation. In *Proceedings of the 11th ACM conference on Computer and communications security*, pages 132–145, 2004.

[11] Ernie Brickell, Liqun Chen, and Jiangtao Li. A new direct anonymous attestation scheme from bilinear maps. In *Trusted Computing-Challenges and Applications: First International Conference on Trusted Computing and Trust in Information Technologies, Trust 2008 Villach, Austria, March 11-12, 2008 Proceedings 1*, pages 166–178. Springer, 2008.

[12] Ernie Brickell and Jiangtao Li. Enhanced privacy id: A direct anonymous attestation scheme with enhanced revocation capabilities. In *Proceedings of the 2007 ACM workshop on Privacy in electronic society*, pages 21–30, 2007.

[13] Jan Camenisch, Manu Drijvers, and Anja Lehmann. Anonymous attestation using the strong diffie hellman assumption revisited. In *Trust and Trustworthy Computing: 9th International Conference, TRUST 2016, Vienna, Austria, August 29-30, 2016, Proceedings 9*, pages 1–20. Springer, 2016.

[14] David L Chaum. Untraceable electronic mail, return addresses, and digital pseudonyms. *Communications of the ACM*, 24(2):84–90, 1981.

[15] Jack Choquette. Nvidia hopper gpu: Scaling performance. In *2022 IEEE Hot Chips 34 Symposium (HCS)*, pages 1–46. IEEE Computer Society, 2022.

[16] Amrita Roy Chowdhury, Chuan Guo, Somesh Jha, and Laurens van der Maaten. Eiffel: Ensuring integrity for federated learning, 2022.

[17] Fabiana Clemente, Gonçalo Martins Ribeiro, Alexandre Quemy, Miriam Seoane Santos, Ricardo Cardoso Pereira, and Alex Barros. ydata-profiling: Accelerating data-centric ai with high-quality data. *Neurocomputing*, 554:126585, 2023.

[18] Cloudlab. <https://www.cloudlab.us/>.

[19] NVIDIA Corporation. Nsight systems - system-wide performance analysis tool, 2025. Accessed: April 10, 2025.

[20] ByBrian Coutinho. Dynolog: Open source system observability. <https://developers.facebook.com/blog/post/2022/11/16/dynolog-open-source-system-observability/>.

[21] William J. Dally, Stephen W. Keckler, and David B. Kirk. Evolution of the graphics processing unit (gpu). *IEEE Micro*, 41(6):42–51, 2021.

[22] I. Damgård, M. Jurik, and J.B. Nielsen. A generalisation of paillier’s public-key system with applications to electronic voting. *Int. J. Inf. Sec.*, 2010.

[23] Datadog. Datadog continuous profiler. <https://www.datadoghq.com/product/code-profiling/>.

[24] Michael Davies, Ian McDougall, Selvaraj Anandaraj, Deep Machchhar, Rithik Jain, and Karthikeyan Sankaralingam. A journey of a 1,000 kernels begins with a single step: A retrospective of deep learning on gpus. In *Proceedings of the 29th ACM International Conference on Architectural Support for Programming Languages and Operating Systems, Volume 2*, pages 20–36, 2024.

[25] Roger Dingledine, Nick Mathewson, Paul F Syverson, et al. Tor: The second-generation onion router. In *USENIX security symposium*, volume 4, pages 303–320, 2004.

[26] Equinix. m3.small.x86. specifications & pricing <https://deploy.equinix.com/product/servers/m3-small/>.

[27] Ulfar Erlingsson, Vasya Pihur, and Aleksandra Korolova. Rappor: Randomized aggregatable privacy-preserving ordinal response. In *CCS*, 2014.

[28] Irene Giacomelli, Somesh Jha, Marc Joye, C. David Page, and Kyonghwan Yoon. Privacy-preserving ridge regression with only linearly-homomorphic encryption. *Cryptology ePrint Archive*, Paper 2017/979, 2017. <https://eprint.iacr.org/2017/979>.

[29] Irene Giacomelli, Somesh Jha, Marc Joye, C David Page, and Kyonghwan Yoon. Privacy-preserving ridge regression with only linearly-homomorphic encryption. In *Applied Cryptography and Network Security (ACNS)*, 2018.

[30] Open telemetry. <https://cloud.google.com/learn/what-is-opentelemetry>.

[31] Grafana. Pyroscope. <https://github.com/grafana/pyroscope>.

[32] Paul Grubbs, Marie-Sarah Lacharite, Brice Minaud, and Kenneth G Paterson. Learning to reconstruct: Statistical learning theory and encrypted database attacks. In *IEEE Symposium on Security and Privacy (SP)*, 2019.

[33] Greg Hamerly, Erez Perelman, Jeremy Lau, and Brad Calder. Simpoint 3.0: Faster and more flexible program phase analysis. *Journal of Instruction Level Parallelism*, 7(4):1–28, 2005.

[34] Yueming Hao, Xu Zhao, Bin Bao, David Berard, Will Constable, Adnan Aziz, and Xu Liu. Torch-bench: Benchmarking pytorch with high api surface coverage. *arXiv preprint arXiv:2304.14226*, 2023.

[35] Radek Hranický, Lukáš Zobal, Ondřej Ryšavý, and Dušan Kolář. Distributed password cracking with boinc and hashcat. *Digital Investigation*, 30:161–172, 2019.

[36] Apple Inc. About icloud private relay, 2023. Accessed: April 10, 2025.

[37] Intel. Intel continuous profiler. <https://www.intel.com/news-events/press-releases/detail/1683/intel-releases-continuous-profiler-to-increase-cpu>.

[38] Intel. Intel paillier cryptosystem library. <https://github.com/intel/pailliercryptolib/tree/development>.

[39] Simon Johnson, Vinnie Scarlata, Carlos Rozas, Ernie Brickell, Frank McKeen, et al. Intel software guard extensions: Epid provisioning and

attestation services. *White Paper*, 1(1-10):119, 2016.

[40] Svilen Kanev, Juan Pablo Darago, Kim Hazelwood, Parthasarathy Ranganathan, Tipp Moseley, Gu-Yeon Wei, and David Brooks. Profiling a warehouse-scale computer. In *Proceedings of the 42nd Annual International Symposium on Computer Architecture*, pages 158–169, 2015.

[41] Jonathan Katz and Yehuda Lindell. *Introduction to Modern Cryptography: Third Edition*. Chapman & Hall/CRC Cryptography and Network Security Series) 3rd Edition, 2020.

[42] Tanvir Ahmed Khan, Nathan Brown, Akshitha Sriraman, Niranjan K Soundararajan, Rakesh Kumar, Joseph Devietti, Sreenivas Subramoney, Gilles A Pokam, Heiner Litz, and Baris Kasikci. Twig: Profile-guided btb prefetching for data center applications. In *MICRO-54: 54th Annual IEEE/ACM International Symposium on Microarchitecture*, pages 816–829, 2021.

[43] Tanvir Ahmed Khan, Ian Neal, Gilles Pokam, Barzan Mozafari, and Baris Kasikci. Dmon: Efficient detection and correction of data locality problems using selective profiling. In *15th {USENIX} Symposium on Operating Systems Design and Implementation ({OSDI} 21)*, pages 163–181, 2021.

[44] Jeremy Lau, Erez Perelman, and Brad Calder. Selecting software phase markers with code structure analysis. In *International Symposium on Code Generation and Optimization (CGO’06)*, pages 12–pp. IEEE, 2006.

[45] Jeremy Lau, Stefan Schoemakers, and Brad Calder. Structures for phase classification. In *IEEE International Symposium on-ISPASS Performance Analysis of Systems and Software, 2004*, pages 57–67. IEEE, 2004.

[46] Brian Neil Levine, Clay Shields, and N Boris Margolin. A survey of solutions to the sybil attack. *University of Massachusetts Amherst, Amherst, MA*, 7:224, 2006.

[47] Tyler Lubeck. Distributed password cracking with john the ripper. Technical report, Tufts University, 2013.

[48] Chiara Marcolla, Victor Sucasas, Marc Manzano, Riccardo Bassoli, Frank H.P. Fitzek, and Najwa Aaraj. Survey on fully homomorphic encryption, theory, and applications. *Cryptology ePrint Archive*, Paper 2022/1602, 2022.

[49] Will constable et al. 2020. torchbench: a collection of open source benchmarks for pytorch performance and usability evaluation. <https://github.com/pytorch/benchmark>.

[50] Microsoft. Azure monitor. <https://learn.microsoft.com/en-us/azure/azure-monitor/getting-started>.

[51] Sparsh Mittal and Shraiyyh Vaishay. A survey of techniques for optimizing deep learning on gpus. *Journal of Systems Architecture*, 99:101635, 2019.

[52] Payman Mohassel and Yupeng Zhang. Secureml: A system for scalable privacy-preserving machine learning. In *2017 IEEE Symposium on Security and Privacy (SP)*, pages 19–38, 2017.

[53] Arvind Narayanan and Vitaly Shmatikov. Robust de-anonymization of large sparse datasets. In *IEEE Symposium on Security and Privacy*, 2008.

[54] V. Nikolaenko, U. Weinsberg, S. Ioannidis, M. Joye, D. Boneh, and N. Taft. Privacy-preserving ridge regression on hundreds of millions of records. In *IEEE Symposium on Security and Privacy*, 2013.

[55] NVIDIA. Geforce experience. <https://www.nvidia.com/en-us/geforce/geforce-experience/>.

[56] Gpu accelerated libraries. <https://developer.nvidia.com/gpu-accelerated-libraries>.

[57] NVIDIA. Kernel profiling guide. <https://docs.nvidia.com/nsight-compute/ProfilingGuide/index.html#metrics-structure>.

[58] NVIDIA. NVIDIA H100 Tensor Core GPU Architecture. <https://resources.nvidia.com/en-us-tensor-core/gtc22-whitepaper-hopper>.

[59] P. Paillier. Public-key cryptosystems based on composite degree residuosity classes. In *Advances in Cryptology (EUROCRYPT)*, 1999.

[60] Andrew Paverd, Andrew Martin, and Ian Brown. Modelling and automatically analysing privacy properties for honest-but-curious adversaries. *Tech. Rep.*, 2014.

[61] Ania M. Piotrowska, Jamie Hayes, Tariq Elahi, Sebastian Meiser, and George Danezis. The loopix anonymity system. In *26th USENIX Security Symposium (USENIX Security 17)*, pages 1199–1216, Vancouver, BC, August 2017. USENIX Association.

[62] Raluca Ada Popa, Catherine M. S. Redfield, Nickolai Zeldovich, and Hari Balakrishnan. Cryptdb: Protecting confidentiality with encrypted query processing. In *In Proceedings of the 23rd ACM Symposium on Operating Systems Principles (SOSP)*, October 2011.

[63] Microsoft Research. <https://www.microsoft.com/en-us/research/group/privacy-preserving-machine-learning-innovation/>, 2024.

[64] Zahra Rezapour Siahgourabi. Autocpa: Automatic continuous profiling and analysis. Master’s thesis, University of Waterloo, 2020.

[65] Miraqa Safi. Distributive continuous profiling for iot devices. 2021.

[66] Patrick Sattler, Juliane Aulbach, Johannes Zirngibl, and Georg Carle. Towards a tectonic traffic shift? investigating apple’s new relay network. *arXiv preprint arXiv:2207.02112*, 2022.

[67] Korakit Seemakhupt, Brent E Stephens, Samira Khan, Sihang Liu, Hassan Wassel, Soheil Hassas Yeganeh, Alex C Snoeren, Arvind Krishnamurthy, David E Culler, and Henry M Levy. A cloud-scale characterization of remote procedure calls. In *Proceedings of the 29th Symposium on Operating Systems Principles*, pages 498–514, 2023.

[68] Han Shen, Krzysztof Pszeniczny, Rahman Lavaee, Snehasish Kumar, Sriraman Tallam, and Xinliang David Li. Propeller: A profile guided, relinking optimizer for warehouse-scale applications. In *Proceedings of the 28th ACM International Conference on Architectural Support for Programming Languages and Operating Systems, Volume 2*, pages 617–631, 2023.

[69] Timothy Sherwood, Erez Perelman, and Brad Calder. Basic block distribution analysis to find periodic behavior and simulation points in applications. In *Proceedings 2001 International Conference on Parallel Architectures and Compilation Techniques*, pages 3–14. IEEE, 2001.

[70] Timothy Sherwood, Erez Perelman, Greg Hamerly, and Brad Calder. Automatically characterizing large scale program behavior. *ACM SIGPLAN Notices*, 37(10):45–57, 2002.

[71] Timothy Sherwood, Erez Perelman, Greg Hamerly, Suleyman Sair, and Brad Calder. Discovering and exploiting program phases. *IEEE micro*, 23(6):84–93, 2003.

[72] Timothy Sherwood, Suleyman Sair, and Brad Calder. Phase tracking and prediction. *ACM SIGARCH Computer Architecture News*, 31(2):336–349, 2003.

[73] Polar Signals. parca. <https://github.com/parca-dev/parca>.

[74] Splunk. Splunk alwayson profiling. <https://docs.splunk.com/observability/en/apm/profiling/intro-profiling.html>.

[75] Akshitha Sriraman and Abhishek Dhanotia. Accelerometer: Understanding acceleration opportunities for data center overheads at hyperscale. In *Proceedings of the Twenty-Fifth International*

*Conference on Architectural Support for Programming Languages and Operating Systems*, pages 733–750, 2020.

[76] Haifeng Sun, Jiaheng Li, Jintao He, Jie Gui, and Qun Huang. Omnipiwindow: A general and efficient window mechanism framework for network telemetry. In *Proceedings of the ACM SIGCOMM 2023 Conference*, pages 867–880, 2023.

[77] Nicolas T. Bitcoin - putting its colossal computing power into perspective, 2024. Accessed: April 10, 2025.

[78] Zhiyi Tian, Lei Cui, Jie Liang, and Shui Yu. A comprehensive survey on poisoning attacks and countermeasures in machine learning. *ACM Computing Surveys*, 2022.

[79] Tor metrics. <https://metrics.torproject.org/bandwidth.html>.

[80] Alexandru Uta, Alexandru Custura, Dmitry Dulyakin, Ivo Jimenez, Jan Rellermeyer, Carlos Maltzahn, Robert Ricci, and Alexandru Iosup. Is big data performance reproducible in modern cloud networks? In *17th USENIX symposium on networked systems design and implementation (NSDI 20)*, pages 513–527, 2020.

[81] Lingmei Weng, Yigong Hu, Peng Huang, Jason Nieh, and Junfeng Yang. Effective performance issue diagnosis with value-assisted cost profiling. In *Proceedings of the Eighteenth European Conference on Computer Systems*, pages 1–17, 2023.

[82] Runhua Xu, Nathalie Baracaldo, and James Joshi. Privacy-preserving machine learning: Methods, challenges and directions, 2021.

[83] Yikai Zhao, Kaicheng Yang, Zirui Liu, Tong Yang, Li Chen, Shiyi Liu, Naiqian Zheng, Ruixin Wang, Hanbo Wu, Yi Wang, and Nicholas Zhang. LightGuardian: A Full-Visibility, lightweight, in-band telemetry system using sketchlets. In *18th USENIX Symposium on Networked Systems Design and Implementation (NSDI 21)*, pages 991–1010. USENIX Association, April 2021.

[84] Úlfar Erlingsson, Vitaly Feldman, Ilya Mironov, Ananth Raghunathan, Kunal Talwar, and Abhradeep Thakurta. Amplification by shuffling: From local to central differential privacy via anonymity, 2020.